EVOLUTION AND INFLEXIONAL INSTABILITY OF TWISTED MAGNETIC FLUX TUBES

RENZO L. RICCA
Department of Mathematics, University College London, Gower Street, London WC1E 6BT, U.K.

(Received 30 December 1996; accepted 28 January 1997)

Abstract. This paper presents new results concerning evolution and inflexional instability of twisted magnetic flux tubes in the solar corona. Inflexional configurations, attained when the curvature of the tube axis vanishes, are generally present in coronal magnetic structures and are invariably associated with the early stages of kink formation. New equations for the Lorentz force in orthogonal curvilinear coordinates are applied to study the behaviour of twisted flux tubes in presence of inflexion points. We find that inflexional flux tubes are in disequilibrium and evolve spontaneously to inflexion-free configurations, possibly in braid form. These results have important applications for solar coronal structures. First, they prove that the evolution and relaxation of twisted magnetic fields into braid form is a generic feature, confirming the observational evidence of highly twisted and braided structures present in the solar corona. Secondly, they demonstrate that inflexions can trigger kink instabilities, providing a fundamental mechanism for modeling outbreaks of energy into heat, emitted by flares, microflares and mass ejections.

1. Dynamics of Twisted Magnetic Flux Tubes in Orthogonal Curvilinear Coordinates

Highly tangled and braided plasma loops constitute a basic structural element of solar and stellar atmospheres (House and Berger, 1987; Bray *et al.*, 1991). Recent observational measurements (Keller, 1992) confirm that on the Sun, more than 90% of the magnetic flux outside sunspots is concentrated into small and intense flux loops (Spruit and Roberts, 1983). Their structure outlines the entanglement of magnetic lines moved about by the photospheric turbulent flow, whose vortical motion is responsible for the complex topology of the lines of force. For typical solar corona parameters, magnetic Reynolds numbers are very high (of the order of 10^6–10^9), so that resistive and diffusive effects can be neglected. Hence, the evolution of coronal magnetic structures can be studied by ideal magnetohydrodynamics equations.

Twisted magnetic flux tubes can be considered fundamental constituents of complex coronal structures. Their dynamics is governed by the Lorentz force associated with the magnetic field distribution. Here, we present new equations for this force based on appropriate orthogonal curvilinear coordinates that take into account torsion and internal twist of field lines. We take the orthogonal basis $(\hat{\mathbf{e}}_r, \hat{\mathbf{e}}_\theta, \hat{\mathbf{t}})$ given by radial, azimuthal and axial unit vectors centred on the tube axis $\mathbf{X} = \mathbf{X}(s)$ (s arc-length and $\hat{\mathbf{t}}$ tangent to $\mathbf{X}$) and independent coordinates r, ϑ_R, s. The flux tube is identified with a geometric tube of circular cross-section of radius

Solar Physics **172:** 241–248, 1997.

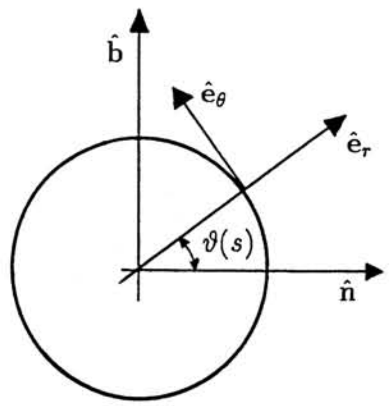

Figure 1. Reference systems centred on the circular cross-section of the flux tube. Note that the azimuthal coordinate θ is a function of the total torsion through Equation (2).

$a < R$, with $R \equiv c^{-1}$ radius of curvature of the tube axis. The tube thinness parameter is given by $\epsilon = r/R < 1$ (not necessarily $\epsilon \ll 1$). The magnetic field $\mathbf{B} = \mathbf{B}_m + \mathbf{B}_a$ is given by a meridian (i.e., poloidal) component $\mathbf{B}_m$ and an axial (i.e., toroidal) component $\mathbf{B}_a$, with

$$\mathbf{B}_m = [0, B_\theta(r, \vartheta(s)), 0], \quad \mathbf{B}_a = [0, 0, B_s(r)] , \tag{1}$$

and B_θ and B_s smooth functions of the radius of the cross-section r $(0 \le r \le a)$ and the azimuth angle $\vartheta = \vartheta(s)$ $(0 \le \vartheta \le 2\pi)$. The independent azimuthal coordinate ϑ_R is related to ϑ by the equation

$$\vartheta(s) = \vartheta_R - \int_0^s \tau(\xi)\,\mathrm{d}\xi , \tag{2}$$

where τ is the torsion of the tube axis. It can be readily verified that the reference system is orthogonal (Mercier, 1963), with scale factors $h_r = 1$, $h_\vartheta = r$ and $h_s = K = 1 - cr\cos\vartheta$. By using the standard Frenet frame, we write the radial and azimuthal unit vectors as $\hat{\mathbf{e}}_r = \hat{\mathbf{n}}\cos\vartheta + \hat{\mathbf{b}}\sin\vartheta$ and $\hat{\mathbf{e}}_\theta = -\hat{\mathbf{n}}\sin\vartheta + \hat{\mathbf{b}}\cos\vartheta$, where $\hat{\mathbf{n}}$ and $\hat{\mathbf{b}}$ are the normal and binormal unit vectors to the tube axis (Figure 1).

The Lorentz force is given by $\mathbf{F} = \mathbf{J} \times \mathbf{B}$, where $\mathbf{J} = \nabla \times \mathbf{B}$ is the current density and, by appropriate rescaling, the magnetic permeability μ is set equal to one. By standard vector calculus the Lorentz force is rewritten as

$$\mathbf{F} = (\nabla \times \mathbf{B}) \times \mathbf{B} = (\mathbf{B} \cdot \nabla)\mathbf{B} - \tfrac{1}{2}\nabla(\mathbf{B}^2) . \tag{3}$$

The r.h.s. of (3) is calculated in the orthogonal reference $(\hat{\mathbf{e}}_r, \hat{\mathbf{e}}_\theta, \hat{\mathbf{t}})$. To evaluate the gradients of the magnetic field in the poloidal and toroidal direction we use Frenet–Serret formulae and the divergence-free condition $\nabla \cdot \mathbf{B} = 0$. From the latter, we have

$$\frac{\partial B_\theta}{\partial \vartheta_R} = -B_\theta \frac{cr}{K} \sin\vartheta \,, \tag{4}$$

where we made use of (2). After some algebra, we can write the Lorentz force explicitly in terms of radial, meridian and axial components, i.e., $\mathbf{F} = \mathbf{F}_r + \mathbf{F}_m + \mathbf{F}_a$, where

$$\mathbf{F}_r = F_r \hat{\mathbf{e}}_r = \left[{B_s}^2 \frac{c}{K} \cos\vartheta - \frac{{B_\theta}^2}{r} - \frac{1}{2}\frac{\partial}{\partial r}\left({B_\theta}^2 + {B_s}^2\right) \right] \hat{\mathbf{e}}_r \,, \tag{5}$$

$$\mathbf{F}_m = F_\vartheta \hat{\mathbf{e}}_\theta = B_s \frac{c}{K} \sin\vartheta \left(B_\theta \frac{r\tau}{K} - B_s \right) \hat{\mathbf{e}}_\theta \,, \tag{6}$$

$$\mathbf{F}_a = F_s \hat{\mathbf{t}} = B_\theta \frac{c}{K} \sin\vartheta \left(B_s - B_\theta \frac{r\tau}{K} \right) \hat{\mathbf{t}} \,. \tag{7}$$

Radial and meridian components can be re-arranged in terms of a component perpendicular to the tube axis ($\mathbf{F}_\perp$) and the poloidal component ($\mathbf{F}_p$), given by

$$\mathbf{F}_\perp = {B_s}^2 \frac{c}{K} \hat{\mathbf{n}} - \left[\frac{{B_\theta}^2}{r} + \frac{1}{2}\frac{\partial}{\partial r}\left({B_\theta}^2 + {B_s}^2\right) \right] \hat{\mathbf{e}}_r \,, \tag{8}$$

$$\mathbf{F}_p = B_\theta B_s \frac{cr\tau}{K^2} \sin\vartheta \hat{\mathbf{e}}_\theta \,. \tag{9}$$

The flux tube moves in the plasma by the action of the perpendicular component (8), given by the curvature contribution along the normal direction (note the presence of the scale factor K) balanced by the contribution from magnetic pressure in the radial direction. For relatively thick flux tubes, i.e., when $\epsilon = O(1)$, the scale factor $K = 1 - cr\cos\vartheta$ may enhance considerably curvature effects. When $\epsilon \ll 1$, $K \approx 1$ and we recover the classical solution for very thin flux tubes. The poloidal component given by (9) has no effect on the tube displacement, but generates a meridian flow, convecting the plasma from the inner concave region towards the outer convex region, with consequential re-arrangement of the magnetic field lines. Note that in absence of the meridian field (zero twist field everywhere) $\mathbf{F}_p = \mathbf{F}_a = 0$. As we should expect $\mathbf{B} \cdot \mathbf{F} = 0$, i.e., the Lorentz force acts normally to the helical path of the twisted field lines, with

$$\frac{|\mathbf{F}_a|}{|\mathbf{F}_m|} = -\frac{B_\theta}{B_s} = -\frac{\Theta r}{KL} \,, \tag{10}$$

which relates magneto-mechanical effects to twist (Θ) and tube geometry (L is the tube length).

2. Inflexional Instability of Twisted Magnetic Flux Tubes

In general knotted magnetic flux tubes exhibit inflexional configurations. The geometry of these configurations is characterized by the presence of points of inflexion (i.e., points where curvature vanishes) along the tube axis. Inflexional states are easily identifiable for plane curves: in this case the inflexional geometry is simply given by an S-shaped curve with the inflexion point at the change of concavity. Inflexional configurations in magnetic field lines, however, are ubiquitous, especially in highly tangled structures. Ricca and Moffatt (1992) showed that the appearance of inflexional states is invariably associated with the continuous exchange of writhe and twist helicity, a recurrent mechanism in solar coronal structures. The dynamics of magnetic flux tubes in inflexional configuration can be studied by applying the above equations to a generic deformation through inflexion. The generic behaviour associated with passage through an inflexional state (say at $s = 0$ and time $t = 0$) has been studied by Ricca and Moffatt (1992), and is given by the time-dependent twisted cubic

$$\mathbf{X}(s,t) = (s - \tfrac{2}{3}t^2 s^3, -ts^2, s^3) \tag{11}$$

for small s and t ($|s| \gg t$), where t denotes some 'kinematical' time (obtained by appropriate rescaling of the real dynamics).

We can now apply Equations (5)–(7) to the inflexional geometry (11). Equilibrium is attained by satisfying the magnetostatic condition $\mathbf{J} \times \mathbf{B} = \nabla p$, which gives

$$\nabla \times \mathbf{F} = 0\,. \tag{12}$$

This analysis is carried out by rewriting Equation (12) in the orthogonal curvilinear basis $(\hat{\mathbf{e}}_r, \hat{\mathbf{e}}_\theta, \hat{\mathbf{t}})$ with inflexional geometry (11). After appropriate non-dimensionalisation of variables and some tedious, but straightforward algebra, we can show (Ricca, 1996a, b) that Equation (12) has no physical solution. Indeed, we can prove that

$$\frac{B_\theta}{B_s} \sim \frac{G}{\cos\vartheta} \quad (B_s \neq 0)\,, \tag{13}$$

where G is a smooth function of the flux tube geometry. From (13) we see that B_θ blows-up as $\sec\vartheta = 1/\cos\vartheta$ at $\vartheta = \pi/2$ and $\vartheta = 3\pi/2$. Note that the singularity is independent of the flux tube thickness ϵ, so that this result holds true for relatively thick flux tubes. Setting torsion to zero (in the function G), we can check that the instability is also present in planar configurations (S-shaped curves), where the disequilibrium is clearly driven by the normal unit vector in the two regions of opposite concavity. We conclude that there is no equilibrium for flux tubes in inflexional configuration.

3. Physical Consequences of Inflexional Instability

The inflexional instability of magnetic flux tubes has important effects on the evolution of coronal magnetic fields. In ideal conditions (that is when viscous or resistive effects are neglected) magnetic fields deform and re-arrange themselves in a continuous fashion by conserving topology (Antiochos, 1987; Moffatt, 1992). Inflexions are removed by a re-arrangement of the field structure into a topologically equivalent configuration, free from inflexions and possibly in braid form. Braids are given by entangled field lines and constitute favoured candidates for solar coronal structures (Berger, 1987). Typically, magnetic tubes re-adjust themselves by reducing the excess of internal twist and magnetic stress, a process that in ideal conditions is known to convert twist helicity into writhe helicity (Moffatt and Ricca, 1992). This process is achieved mechanically by the action of the poloidal component (9) of the Lorentz force on the tube strands. Inflexions are removed either by lowering the internal twist through redistribution of torsional energy, relaxing the whole structure to a braid pattern, or, if it is possible, by converting as much of twist helicity as possible into writhe helicity, with production of large helical structures (arches with low curvature and large coils). On relatively long time-scales these too, under the action of the normal component of the Lorentz force (8), re-adjust themselves to large inflexion-free braids.

Depending on how much twist has being actually built-up in the flux-tube, we may identify three different scenarios for the evolution of coronal loops (see Figure 2).

(i) Sub-critical twist: $\Theta < \Theta_{\rm cr}$. The flux tube is still able to absorb a great deal of twisting from chaotic and vortical motion in the photosphere and surrounding plasma turbulence. Writhe helicity (which is a measure of the number of kinks formed) may increase and is redistributed into twist helicity. The evolution is dominated by curvature forces due to the normal component of Equation (8). These induce a continuous, progressive shortening of the field lines, that is balanced by plasma pressure. Note that for thin flux tubes the contribution from $B_\theta{}^2/r$ is small compared with tension effects. At typical critical twist values ($\Theta_{\rm cr}$) for kink formation (see, for example, Priest, Hood, and Anzer, 1989), we have

$$\frac{B_s{}^2 c/K}{B_\theta{}^2/r} \gg \frac{K}{N^2} = \mathrm{O}(1)\,, \tag{14}$$

where $N = \mathrm{O}(1)$ is the critical number of twist turns for kink instability. In this situation, big arches and large helical structures, with low bending energy, are produced. Inflexions are removed by re-arranging the initial configuration into a braided pattern. Thus, braided coronal loops are formed, with a relatively long lifetime.

(ii) Twist almost at a critical level: $\Theta \approx \Theta_{\rm cr}$. In this case the flux tube has as much twist as it can support, with part of the total helicity converted into writhe helicity.

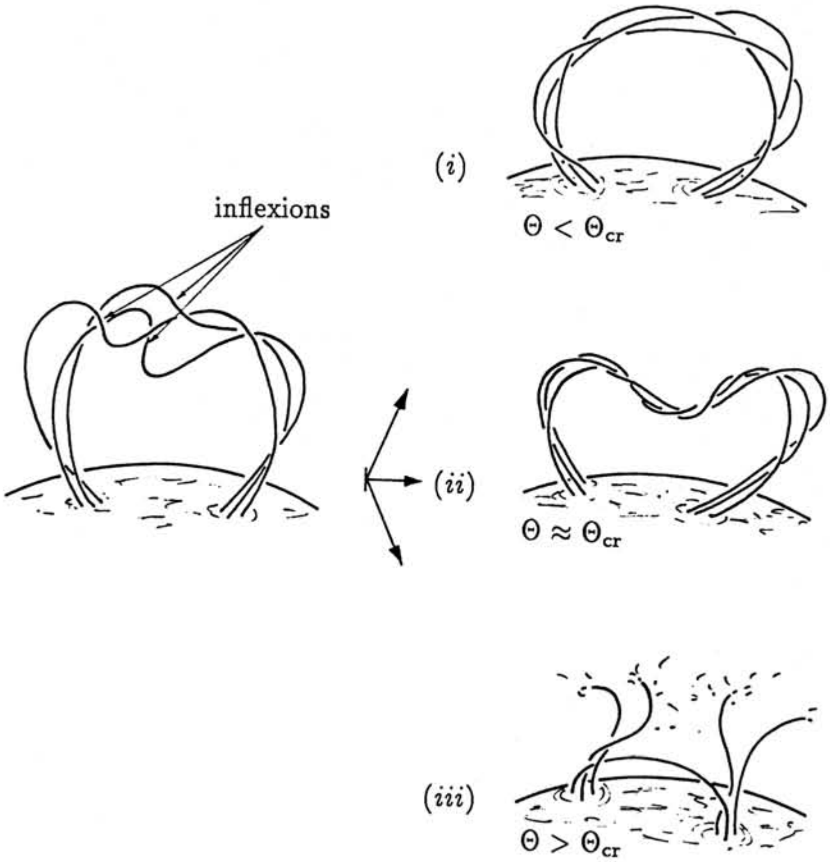

Figure 2. A coronal loop is identified with a bundle of magnetic fields twisted-up by the vortical photospheric motion that during evolution may develop inflexional configurations in disequilibrium. Depending on the amount of twist actually present in the loop, we have: (i) magnetic field lines relaxing into a braid pattern; (ii) flux tube developing a hammock configuration; or (iii) passage through inflexion, triggering kink instability and eventual outbreak of energy.

Writhe values are therefore high, but not high enough for the flux tube to produce a full kink. In this case we can show (Ridgway and Priest, 1993; Ricca, 1994) that coronal loops can attain a full, three-dimensional hammock configuration. This is a particular geometry, where the dip is formed and maintained through the inward action of the Lorentz force (in Equation (5)) on plasma particles. Hammock configurations are good candidates for providing mechanical support for cool, heavier plasma in the corona. Here we should point out that even when the hammock configuration is attained by a magnetic field purely sheared near the photospheric neutral line (see, for example, Antiochos, Dahlburg, and Klimchuk, 1994), twist injected by vortical photospheric motion should still be considered as an influencing factor for dip formation (since shear can always be decomposed into a strain and a twist action).

(iii) Super-critical twist: $\Theta > \Theta_{cr}$. In this case high magnetic tension drives inflexional flux tubes to an abrupt development of a full kink. But in super-critical state, this triggers kink instability (Raadu, 1972). Highly twisted field lines relax suddenly to become narrowly coiled together in a small region of space, where plasma particles are trapped in high density. Here, resistive effects become too important to be neglected and high currents soon develop. Magnetic field topology is no longer conserved, with lines of force undergoing physical reconnections and complete re-structuring (van Ballegooijen, 1985). The flux tube liberates excess of torsional energy by breaking-up, with an out-break of magnetic energy released into heat, to produce flares and erupting prominences (Hood and Priest, 1979).

As we have seen, in all these events inflexional instabilities play an important rôle. Their presence is source of a disequilibrium that leads to re-arrangements or re-structurings of the initial configuration. These results are important for energy estimates of solar coronal structures, especially when these estimates are based on theoretical models that are very sensitive to variations in geometric and topological information (Berger, 1993; Chui and Moffatt, 1995; see also Ricca and Berger, 1996). The accuracy of these estimates is crucial to give precise evaluations of the amount of energy that can be released into heat during flares, microflares, and mass ejections (Parker, 1983). Moreover, the presence of highly twisted and braided magnetic structures in the solar corona (Berger, 1987; Bray *et al.*, 1991) is in perfect agreement with our analysis of the relaxation of magnetic fields to braid form, as we have discussed earlier in this section. Our programme is to pursue further this analysis, by combining topological information and magnetic relaxation techniques in order to carry out accurate estimates of minimum energy levels for braided coronal magnetic structures.

Acknowledgement

Financial support from The Leverhulme Trust is kindly acknowledged.

References

Antiochos, S. K.: 1987, *Astrophys. J.* **312**, 886.
Antiochos, S. K., Dahlburg, R. B., and Klimchuk, J. A.: 1994, *Astrophys. J.* **420**, L41.
Berger, M. A.: 1987, *Astrophys. J.* **323**, 406.
Berger, M. A.: 1993, *Phys. Rev. Letters* **70**, 705.
Bray, R. J., Cram, L. E., Durrant, C. J., and Loughhead, R. E.: 1991, *Plasma Loops in the Solar Corona*, Cambridge University Press, Cambridge.
Chui, A. Y. K. and Moffatt, H. K.: 1995, *Proc. Roy. Soc. London* **A451**, 609.
Hood, A. W. and Priest, E. R.: 1979, *Solar Phys.* **64**, 303.
House, L. L. and Berger, M. A.: 1987, *Astrophys. J.* **323**, 406.
Keller, C. U.: 1992, *Nature* **359**, 307.
Mercier, C.: 1963, *Nuclear Fusion* **3**, 89.
Moffatt, H. K.: 1992, in H. K. Moffatt *et al.* (eds), *Topological Aspects of the Dynamics of Fluids and Plasmas*, Kluwer Academic Publishers, Dordrecht, Holland.

Moffatt, H. K. and Ricca, R. L.: 1992, *Proc. Roy. Soc. London* **A439**, 411.
Parker, E.N.: 1983, *Astrophys. J.* **264**, 642.
Priest, E. R., Hood A. W., and Anzer, U.: 1989, *Astrophys. J.* **344**, 1010.
Raadu, M. A.: 1972, *Solar Phys.* **22**, 425.
Ricca, R. L.: 1994, in G. Belvedere *et al.* (eds) *Poster Papers Presented at the VII European Meeting on Solar Physics*, Catania Astrophysical Observatory, Catania, Italy.
Ricca, R.L.: 1996a, in IUTAM *XIX Int. Cong. Theor. Appl. Mech. – Abstracts*, Kyoto, Japan, p. 94.
Ricca, R. L.: 1996b, submitted.
Ricca, R. L. and Berger, M. A.: 1996, *Phys. Today* **49** (12), 24.
Ricca, R. L. and Moffatt, H. K.: 1992, in H. K. Moffatt *et al.* (eds). *Topological Aspects of the Dynamics of Fluids and Plasmas*, Kluwer Academic Publishers, Dordrecht, Holland.
Ridgway, C. and Priest, E. R.: 1993, *Solar Phys.* **146**, 177.
Spruit, H. C. and Roberts, B.: 1983, *Nature* **304**, 401.
van Ballegoojien, A. A.: 1985, *Astrophys. J.* **298**, 421.